

Tip-enhanced Raman spectroscopy for structural analysis of two-dimensional covalent monolayers synthesized on water and on Au (111)

Journal Article

Author(s):

Zheng, Liqing ; Servalli, Marco ; Schlüter, A. Dieter; Zenobi, Renato 

Publication date:

2019

Permanent link:

<https://doi.org/10.3929/ethz-b-000369790>

Rights / license:

[Creative Commons Attribution-NonCommercial 3.0 Unported](#)

Originally published in:

Chemical Science 10(42), <https://doi.org/10.1039/C9SC03296G>

Funding acknowledgement:

741431 - Nanoscale Vibrational Spectroscopy of Sensitive 2D Molecular Materials (EC)

Electronic Supplementary Information

Tip-enhanced Raman spectroscopy for structural analysis of two-dimensional covalent monolayers synthesized on water and on Au (111)

Li-Qing Zheng,^{†a} Marco Servalli,^{†b} A. Dieter Schlüter^b and Renato Zenobi^{a*}

a. Department of Chemistry and Applied Biosciences, ETH Zurich, Vladimir-Prelog-Weg 3, CH 8093, Switzerland

b. Department of Materials, Institute of Polymer Chemistry, ETH Zurich, Vladimir-Prelog-Weg 5, CH 8093, Switzerland

The vibrational modes of the monomer model compound are shown in Movie S1. The vibrational modes of the polymer model compound are shown in Movie S2.

Table of Contents

1. Preparation of Langmuir monolayers.....	S-2
2. Preparation of substrates and transfer of the monolayers.....	S-2
3. Characterization of the monolayers.....	S-3
a. Isotherm.....	S-3
b. Brewster's angle microscopy.....	S-4
c. AFM.....	S-5
d. <i>In-situ</i> fluorescence spectroscopy.....	S-6
e. SEM.....	S-10
f. Optical <i>microscopy</i>	S-11
4. Raman analysis.....	S-12
a. Optimization of conditions for confocal Raman spectroscopy.....	S12
b. Optimization of conditions for TERS measurement.....	S13
c. TERS spectra analysis.....	S14
d. Polymerization conversion calculation.....	S24
e. Error estimation.....	S24
5. References.....	S-26

1. Preparation of Langmuir monolayers

The details about the synthesis and the NMR characterization of monomer **1** can be found in Marco Servalli et al^[1]. A Langmuir trough (KSV 2000 System 2, Finland) was used to create the monomer and polymer monolayers at the air/water interface.^[1] A platinum Wilhelmy balance was used to monitor the surface pressure. For spreading the monomer **1**, a stock solution (0.25 mg/mL) of a 1:1 solvent mixture of chloroform/cyclohexane was prepared. The solution was spread dropwise at the interface with the use of gas-tight glass microsyringe, typically applied volume of 200 μ L. After a time delay of 30 min that allowed the complete evaporation of the solvent, the barriers were compressed to the desired surface pressure, with a compression rate of 3 mm/min. In-plane polymerization was induced by irradiating the monolayer with a custom made LED lamp of wavelength $\lambda = 385$ nm (1W) for the desired time.

2. Preparation of substrates and transfer of the monolayers

Silicon (Si/SiO₂, Thermo, 285 nm) wafers were sonicated in acetone and ethanol for 15 mins, respectively, to remove the coating of photoresist (10 μ m of AZ9260, Merck Performance Materials GmbH, Germany), and then sonicated in millipore H₂O (3 x 15 min). They were then kept under millipore H₂O until use. TEM grids were used as provided by the manufacturer (PLANO GmbH, Wetzlar, Germany). Freshly template-stripped Au substrates^[2] were used to transfer the monolayer sheet from the air-water interface for TERS measurements. The Au (111) single crystal substrate was purchased from MaTeck (Germany). It was firstly cleaned by repeating Ar-ion sputtering at a pressure of 1×10^{-5} mbar for 30 mins (1.5 KeV), followed by annealing in ultrahigh vacuum (1×10^{-9} mbar) at 500°C until the Au (111) turned dark red. The cleaning procedure was repeated three times.

All Langmuir monolayers were transferred horizontally at constant surface pressure using the Langmuir-Schaefer-technique. To minimize the damage of monolayers during transfer, the monolayer with a substrate beneath was slowly pulled out of the water (transfer rate 0.5 mm/min) and the substrate left to dry overnight. For SEM analysis, the copper grids were carefully placed on the water surface and removed with the help of tweezers.

3. Characterization of the monolayers

a. Isotherm

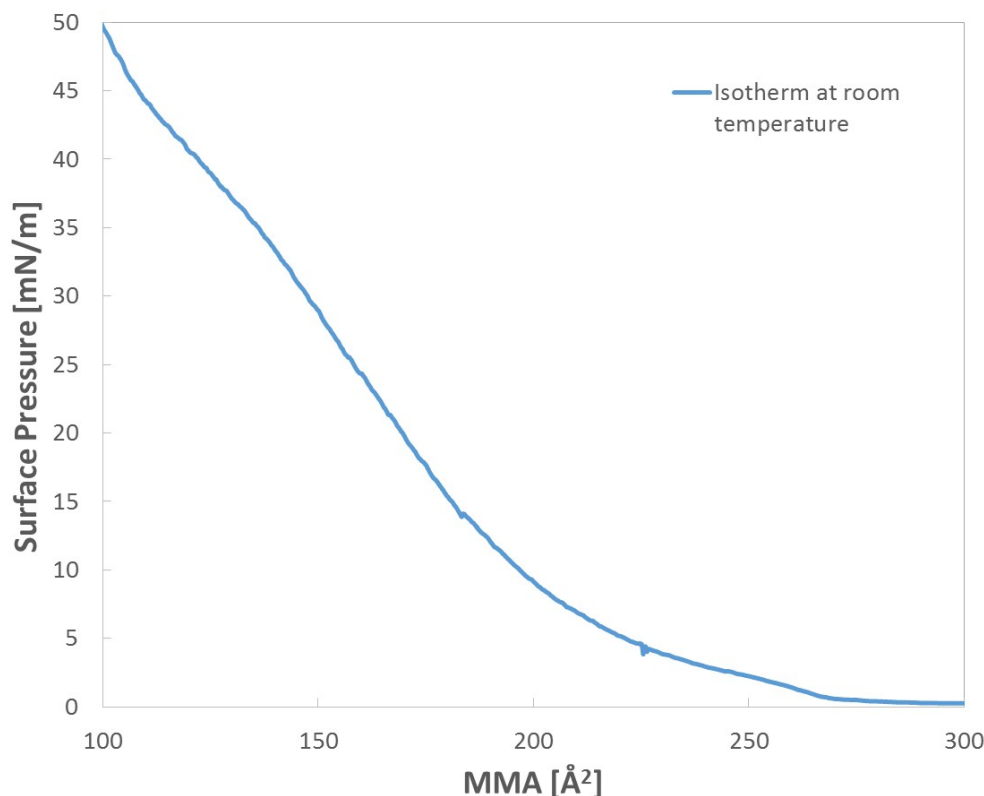


Figure S1. Surface pressure (SP) vs Mean molecular area (MMA) isotherm recorded during compression of a film of monomer **1** at room temperature.

Note: isotherms and MMA values are susceptible to variations between different spreading experiments. Such variations arise from: cleanliness of the water surface, slight differences in the volume spread, contamination of the interface (for instance with dust particles or residual grease particles) and ageing of the monomer stock solution. Factors that can influence the latter are: variation in the concentration due to solvent evaporation from the binary mixture, contamination (dust) and accidental exposure to light, which in solution can cause both photooxidation and dimerization reactions. As such to carry out experiments, the isotherm reproducibility has to be tested over multiple spreading experiments, in order to identify the desired surface pressure and MMA value. The isotherm in Figure S1 is representative for the current study only. Polymerization experiments were carried out aiming at MMA values of around 252 \AA^2 corresponding to a range of pressures from 2 to 7 mN/m. 252 \AA^2 corresponds to the MMA of the desired hexagonal packing ought to provide a 2D polymer, according to DFT simulations.^[1]

b. Brewster's angle microscopy

To visualize the films by Brewster angle microscopy (BAM), a KSV MicroBAM operating with a 659 nm laser and an angle of 53° was used.

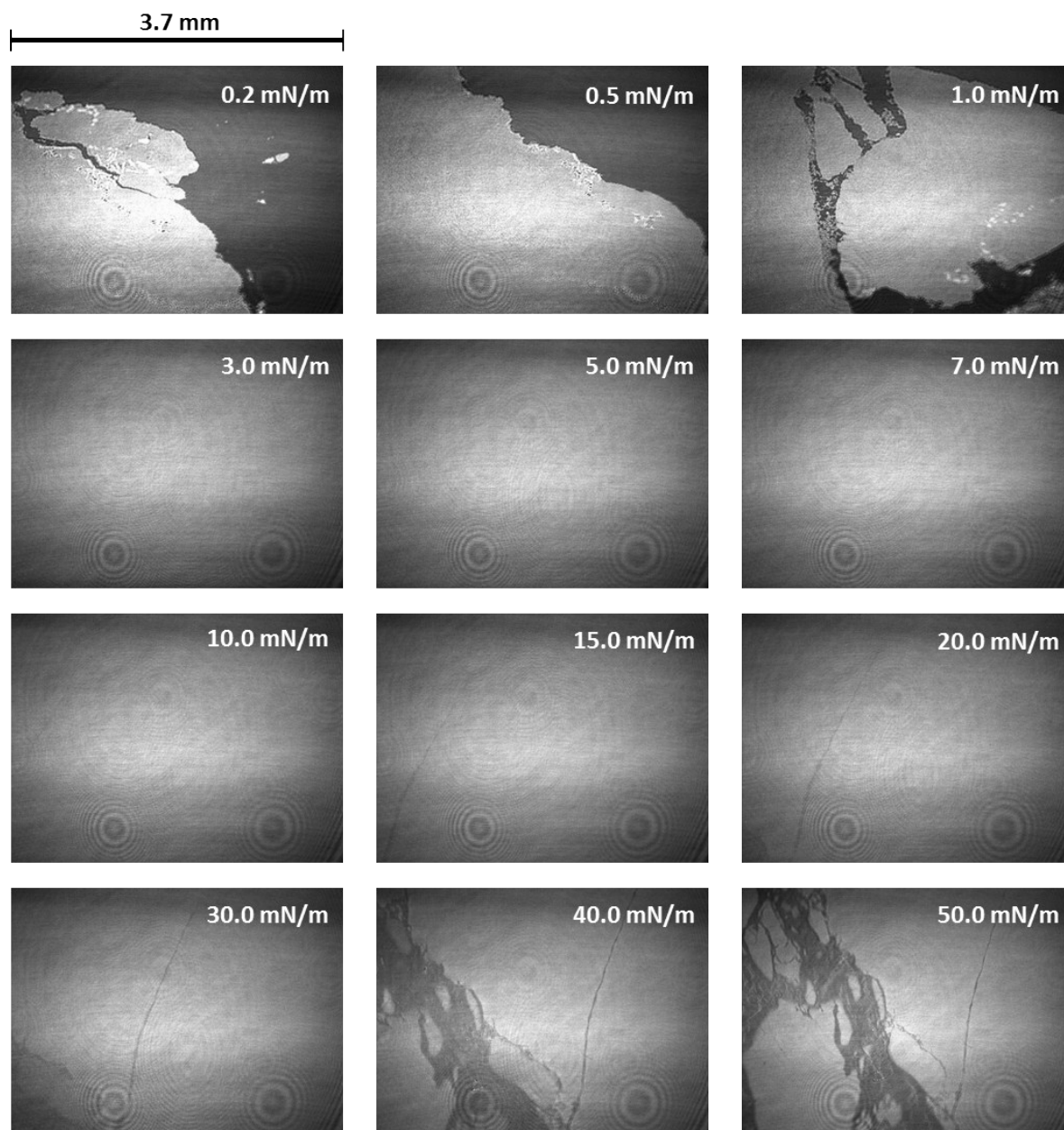


Figure S2. Brewster angle microscopy (BAM) micrographs recorded at different surface pressures during the compression process. The monomer spontaneously self-assembles into homogeneous islands on the water surface, which upon compression coalesce into a continuous monolayer, as can be seen by the monotonous grey contrast. Between SP of 3.0

and 10 mN/m a very homogenous monolayer is observed as shown by the monotonous and uniform grey contrast. At around 30 mN/m and above the film visually starts to collapse. Note: due to automatic adjustment of the contrast in each image, brightness level is only meant to be studied in images individually and not to be compared with other recorded images.

c. AFM

Atomic force microscopy (AFM) measurements were performed using a Nanoscope III Multimode system (Digital Instruments, Santa Barbara, Ca). OMCLAC160TS silicon tips (Olympus, Tokyo, Japan) were used for imaging with a resonance frequency in between 200 and 400 kHz and a spring constant of about 42 N/m (tapping mode). Measurements were performed on 285 nm SiO₂-coated silicon wafers. Height analysis was performed at artificially created step edges (by covering part of the wafers with a piece of freshly cleaved mica before transferring the monolayer).

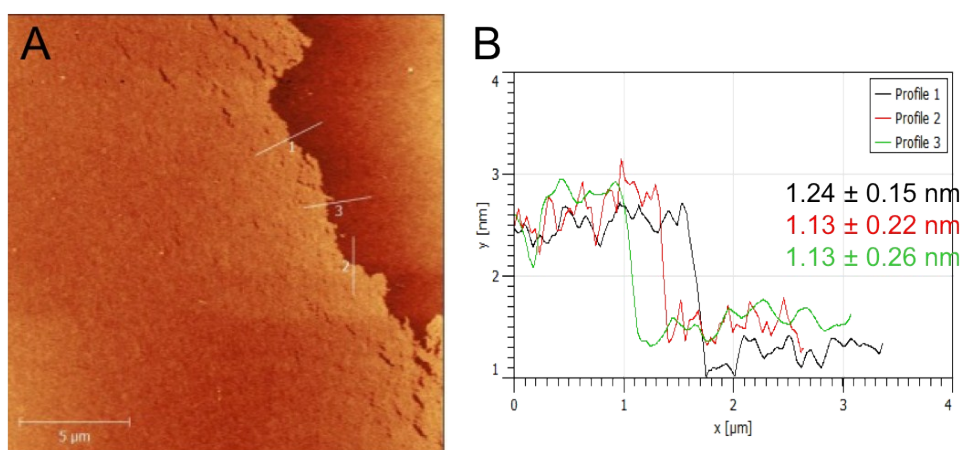


Figure S3. A. Tapping mode AFM image of the monomer film on a SiO₂/Si wafer; B. The corresponding height profiles along the lines indicated in the image.

d. *In-situ* fluorescence spectroscopy

The solution emission spectrum was recorded with a Spex Fluorolog 2 spectrophotometer from Jobin Yvon (United Kingdom) using a quartz cell with a path length of 1 cm. The concentration of the monomer chloroform solution was 2.5 μM . Excitation wavelength was 365 nm.

For recording the emission spectrum from the interface, an Acton series spectrometer from Princeton Instruments (NJ, USA) was used, equipped with an SP-2556 Acton Research 500 mm Imaging Spectrograph (Acton, MA, USA), FC fiber stage and three standard gratings with groove densities of 1200 mm^{-1} , 600 mm^{-1} and 150 mm^{-1} , with blaze size of 500 nm and 68 mm x 68 mm dimensional size. The CCD camera was a Princeton Instruments PIXIS 256E (NJ, USA). The read-out fiber was purchased from AFW Technologies Pty Ltd (Hallam, Australia) and had a core diameter of 50 μm , numerical aperture of 0.12 and FC connectors on both ends. As excitation source, an LED with $\lambda = 365$ nm and with 250 mW power (Omicron Laser, Rodgau, Germany) was used. It was mounted on a lens tube along with a UV fused silica bi-convex lens with 40 mm focal length (Thorlabs, LB4030-UV, Newton, NJ, USA) as well as a band-pass filter transmitting at 370 nm with FWHM of 10 nm (Thorlabs, FB370-10, Newton, NJ, USA). The beam was focused at the interface to produce an illuminating spot with a diameter of about 2 mm. The read-out stage was aligned and focused so to collect as much emission signal as possible. The read-out fiber was fixed on a stage, which was built in-house. A binning of 4 was used to record the data: this value did not affect the resolution of the measurements due to the broad emission spectrum of the monolayer. The CCD read-out was set to the region of interest (ROI), while the ROI set-up on the slit ran from 130 as the start point with a height of 23.

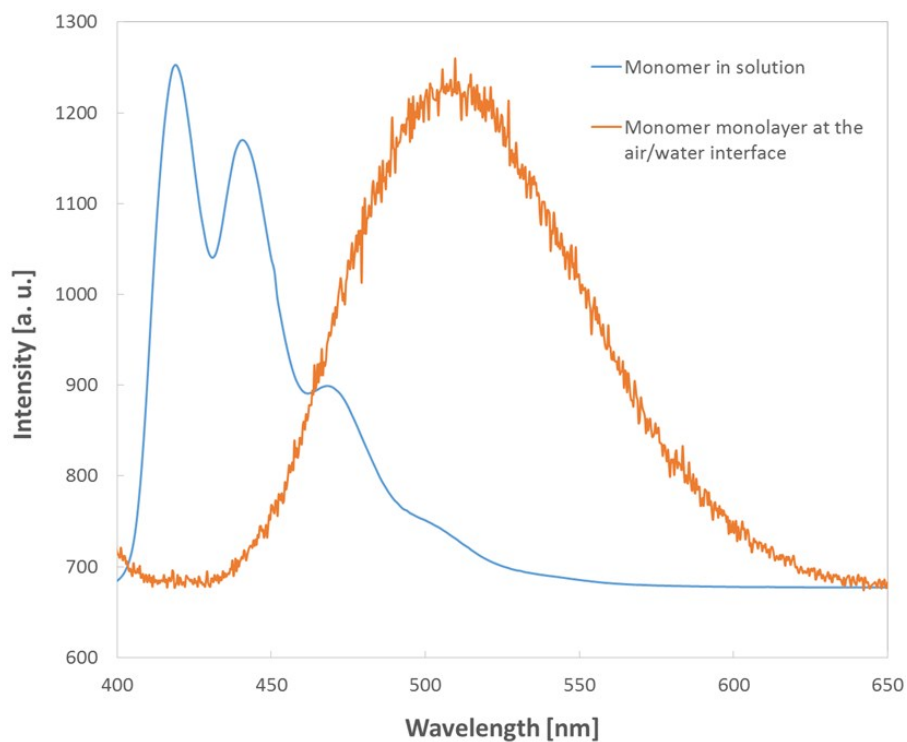


Figure S4. Emission spectra (excitation $\lambda = 365$ nm) of a monomer solution in chloroform (*blue*) and of a monolayer at the air/water interface (*orange*). While in solution the typical vibronic structure of the anthracene units is clearly visible, at the air/water interface there is only a pure excimer emission centered at around 510 nm, indicating face-to-face stacking between the anthracene units of the monomer. No sign of isolated anthracenes is present at the interface. The exposure time was 15 seconds while the LED was at full power during the acquisition time.

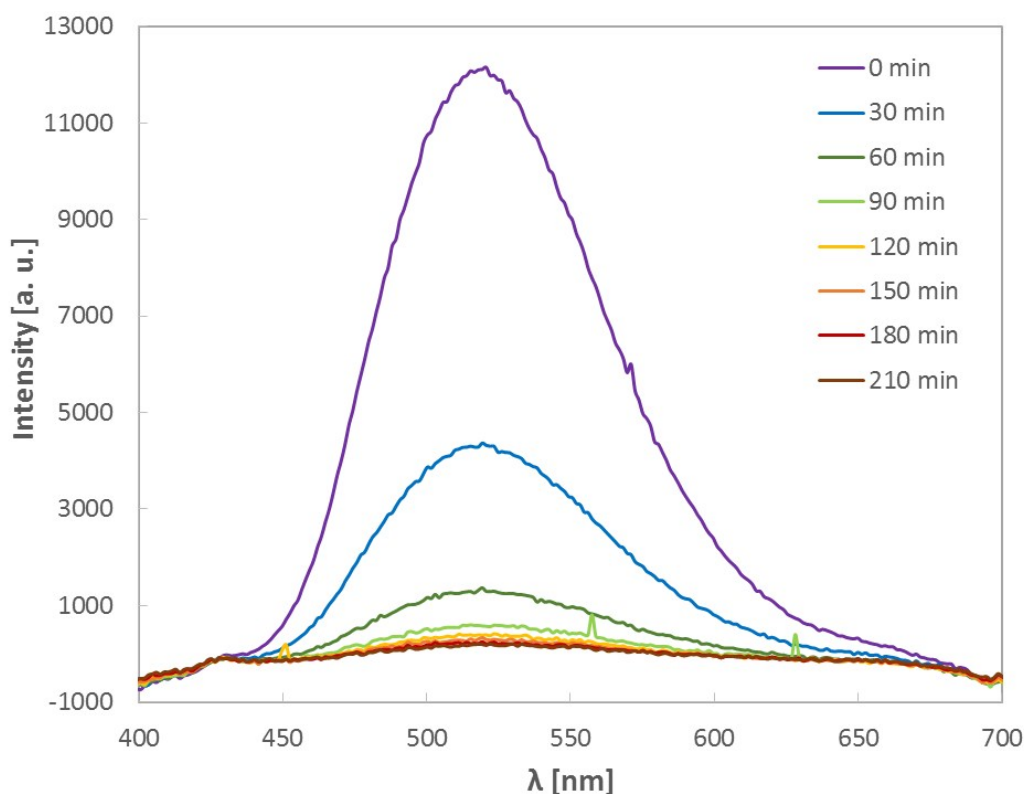


Figure S5. *In-situ* fluorescence decay experiment of a monomer at the air/water interface (for excitation and irradiation a wavelength of 365 nm was chosen); the spectra are baseline corrected. The small spikes in the spectra are due to background radiation. The exposure time was 60s while the LED was at full power during the acquisition time.

Remarks on background subtraction: every emission spectrum carries a signal from Raman scattering of water along with contributions from LED and optics. Moreover, the relatively high exposure time of the CCD camera renders small traces of light visible in the spectrum. It is therefore helpful to subtract such effects. At these exposure times, small defects from the band-pass filter mounted on the LEDs also become visible and need to be taken into account. After a certain time in each experiment, when the excimer signal is decayed significantly, the spectral patterns for long-exposed LED also appears in the measurements. The patterns could be different in terms of intensity due to the changes of the water level upon evaporation. The time-interval at which this pattern is observed, can in fact be taken as the background.

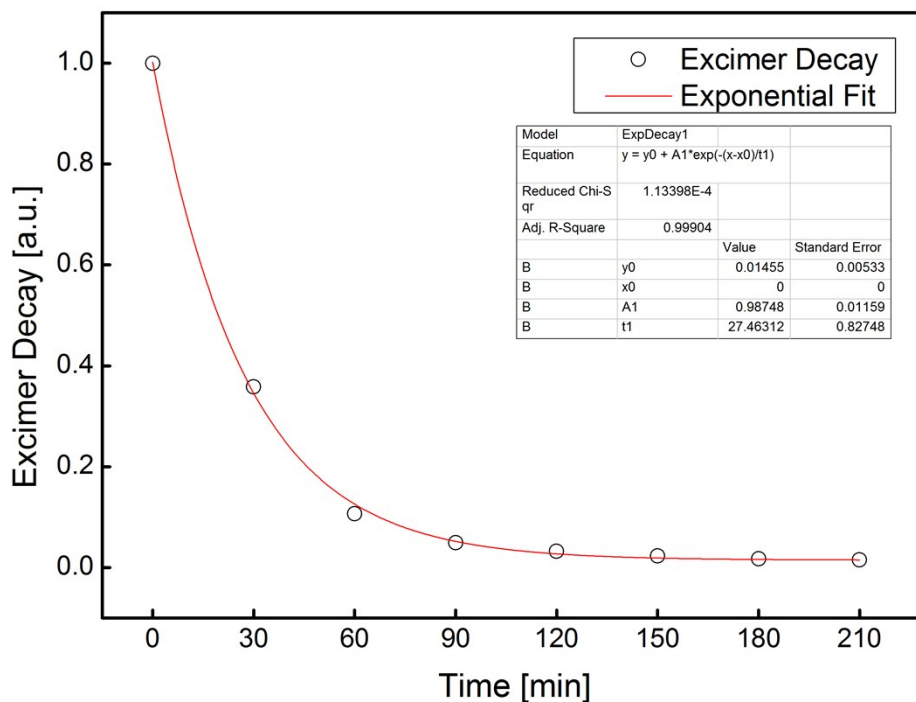


Figure S6. Exponential decay of the excimer fluorescence (λ_{MAX}) displayed in Figure S5. The decay follows first order kinetics and has a half-life of 18.7 min.

Compared to the conversion number calculated according to the *TERS results*, the conversion number calculated based on fluorescence spectroscopy is higher. The difference in the polymerization degree is attributed to two reasons: 1. Two different light sources were used in these two experiments and the distances between the light sources and the samples were also different, therefore the photon flux reaching to the samples is different. 2. After transferring the monolayers of molecules from air/water interface to the Au substrates, we may rupture or fold the sample, leading to the formation of defects.

e. SEM

TEM grids made of copper with the mesh size of 1000 (PLANO, G2780C) were placed on the irradiated spot on the surface of the water. The TEM grids were placed on a PLANO G3662 holder and imaged with FEG-SEM, Zeiss LEO Gemini 1530, Germany, microscope with an in-lens detector.

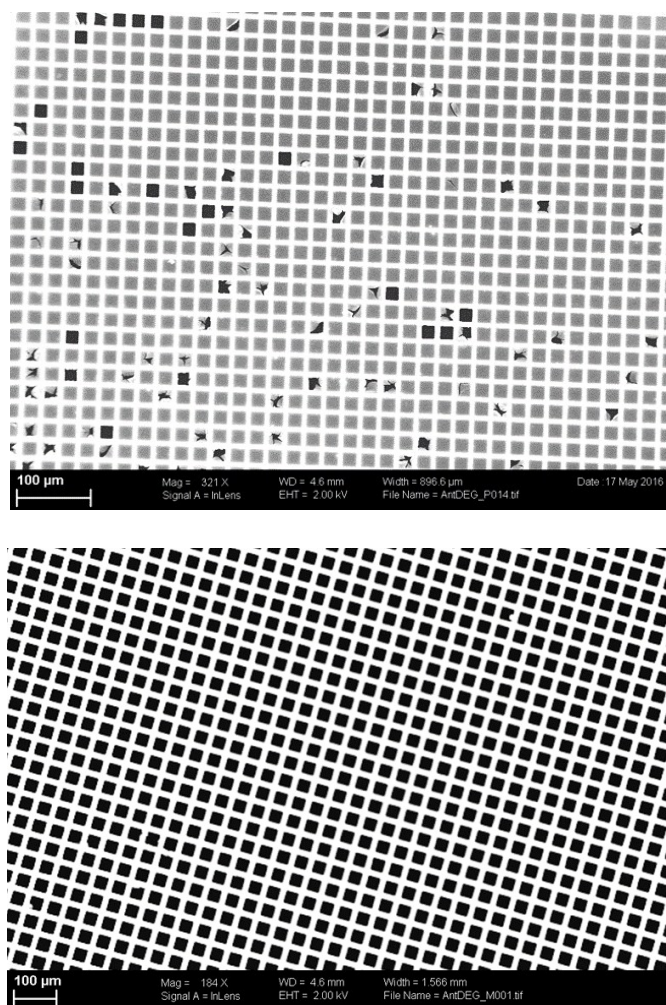


Figure S7. Scanning electron microscopy (SEM) images of a polymerized monolayer (2 h irradiation time) transferred on a copper TEM grids with 20 μm x 20 μm holes (*top*). The monolayer efficiently spans the holes, indicating mechanical coherence of the sheet and a high polymerization conversion. According to bond percolation theory, to achieve mechanical coherence in an hexagonal 6^3 lattice, the polymerization conversion has to be higher than 65%.^[3] Some occasional ruptures arising from the mechanical transfer process can be seen, which provide the necessary contrast to identify the monolayer-covered regions. As control experiment a non-irradiated monomer monolayer was also transferred on a grid and imaged by SEM. The holes appear empty with no spanning visible (*bottom*), indicating the irradiation is necessary to achieve a free-standing monolayer network.

f. Optical microscopy

For optical microscopy, a Leica DM4000M (Leica Microsystems GmbH, Wetzlar, Germany) was used. The monolayers were transferred onto 285 nm SiO₂-coated silicon wafers and visualized in differential interference contrast (DIC) mode.

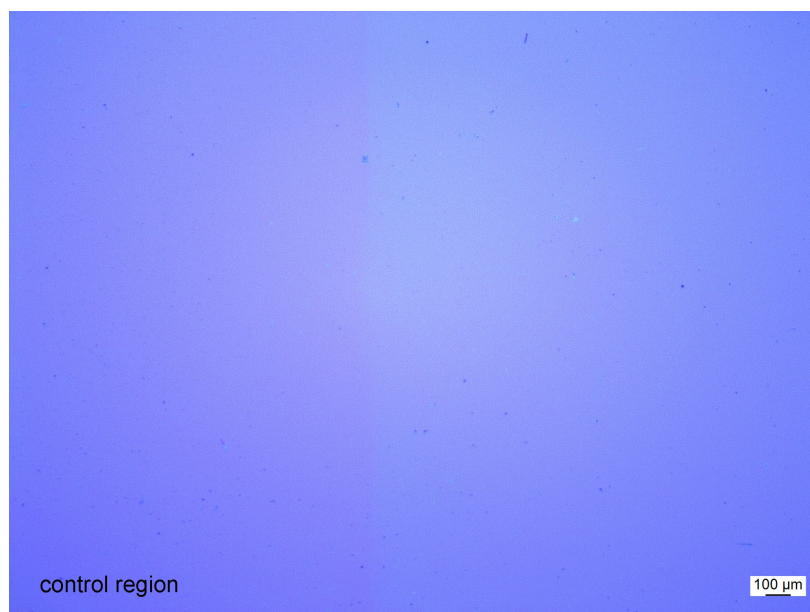


Figure S8. Differential interference contrast microscopy image of a polymerized monolayer (2 h irradiation), transferred on a SiO₂/Si wafer partially covered by a piece of mica. After removal of the mica by tweezers, there is a clear film edge which is located in the middle of the picture. On the right side, the monolayer appears as sky blue in color, whereas the bare silicon oxide surface appears purple. The monolayer homogeneously covers an area of several hundreds of squared micrometers.

4. Raman analysis

a. Optimization of conditions for confocal Raman spectroscopy

Scanning tunneling microscopy (STM) measurements were performed on instruments from NT-MDT (Zelenograd, Russia). An electrochemically etched Ag tip^[4] was used for STM imaging. STM-TERS measurements were performed on a top illumination TERS instrument that combines STM with a Raman spectrometer (NT-MDT, Russia, NTEGRA Spectra Upright). An electrochemically etched Ag tip was used to obtain both the topography and TER spectra. The 632.8 nm He-Ne laser was used as an excitation source. For all the measurements, the tunneling conditions were 200 pA and 1.0 V, the intensity of laser was 30 μ W with 1 s exposure time. Baseline corrections on all of average TER spectra were performed in Origin 9.1 software by the 2nd derivative method with 25 anchor points.

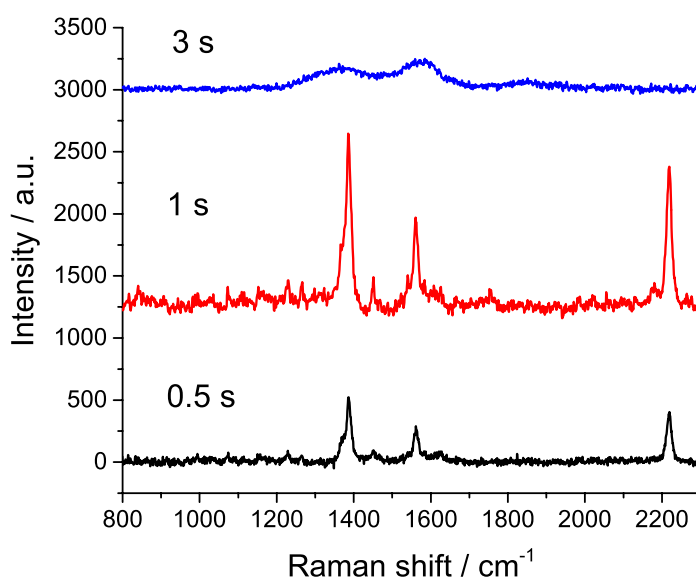


Figure S9. Confocal Raman spectra of monomer **1** powders using different acquisition times at a laser intensity of 2.5 mW.

As shown in Figure S7, the confocal Raman spectrum shows a very good signal-to-noise ratio with only 1 s exposure time at a laser intensity of 2.5 mW. It is in good agreement with the theoretical Raman spectrum (curve a in Figure 1A on manuscript). As the exposure time increased to 3 s, only two broad Raman peaks appear at 1350 cm^{-1} and 1580 cm^{-1} in the spectrum, which indicates that the molecules were decomposed into amorphous carbon by

the irradiation.

b. Optimization of conditions for TERS measurement

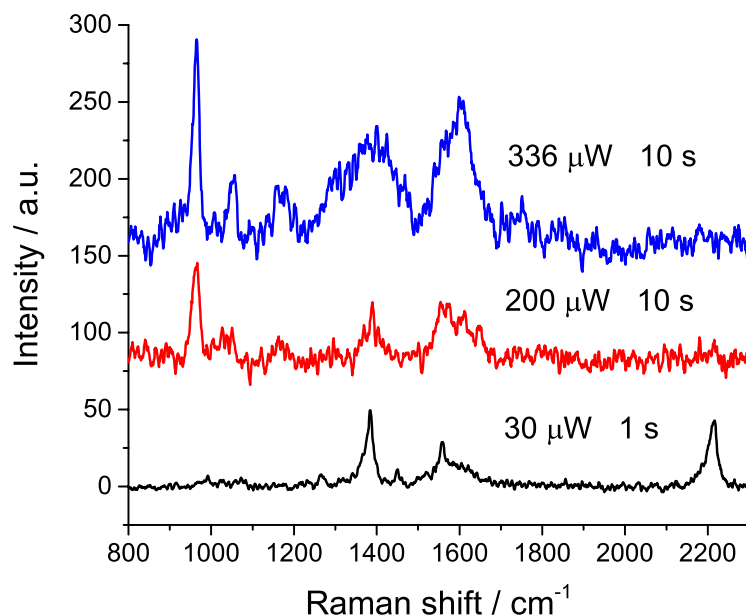


Figure S10. TERS spectra of monomer monolayer on a Au surface using different excitation powers and acquisition times. The tunneling conditions were 200 pA and 1.0 V.

Because the monomer is an insulator,^[1] the Ag tip was kept at a relatively large distance from the monomer sheet to avoid scratches on the sheet, therefore the imposed bias-voltage was 1 V and the tunneling current was only 0.2 nA. A nice TERS spectrum was obtained with only 1 s exposure time at the laser intensity of 30 μW , which is consistent with the confocal Raman spectrum of monomer powders. After increasing the laser power and prolonging acquisition time, we see that the Raman peak at 2215 cm^{-1} disappears. Due to the tip oxidation in air, a new peak appears at 965 cm^{-1} , which was assigned to the sulfate/sulfite ions and/or the respective silver salts.^[5] Moreover, the Raman band at 1385 cm^{-1} got broadened. All these spectral changes indicate that the monolayer sheet had suffered photo-damage. In order to obtain optimal spectra with good signal to noise ratios, 30 μW laser power and 1 s acquisition time were applied for TERS imaging.

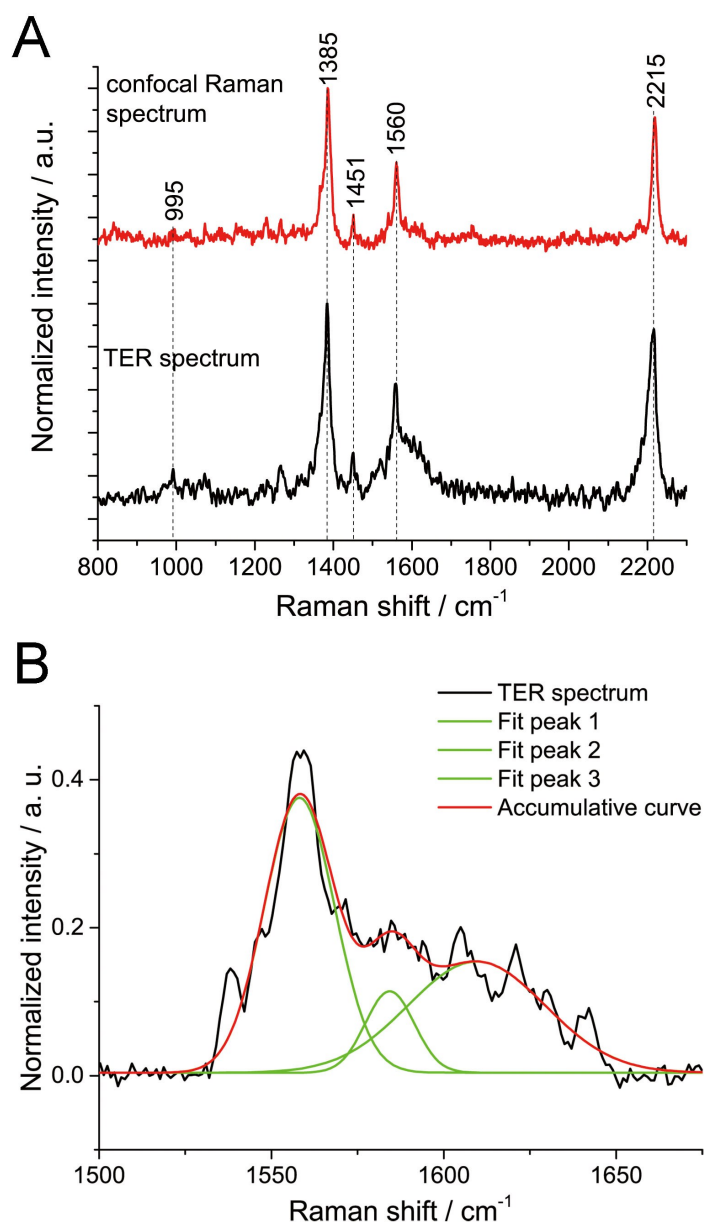


Figure S11. A. Confocal Raman spectrum of monomer powder (red curve) and TER spectrum of monomer monolayer on Au (black curve); B. Gaussian fitting on the peak between 1550 cm^{-1} and 1650 cm^{-1} of the TER spectrum shown in Figure A.

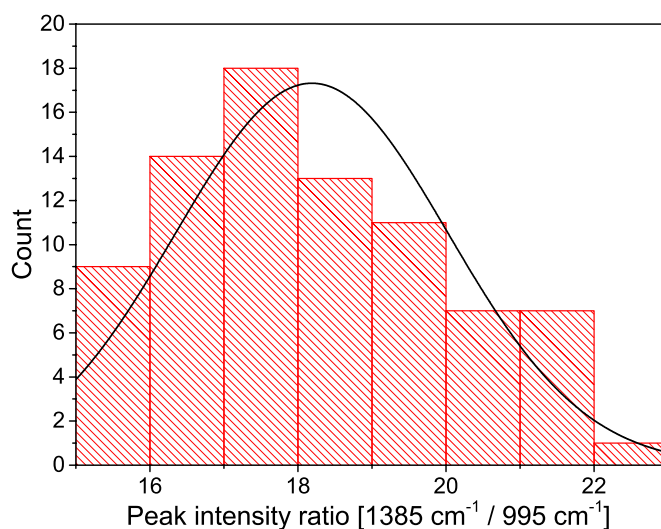


Figure S12. Peak intensity ratio between $1385\text{ cm}^{-1}/995\text{ cm}^{-1}$ distribution of the TER spectra extracted from a TERS map of monomer monolayer. The average peak intensity ratio is 18.2 with 10% spot-to-spot variation.

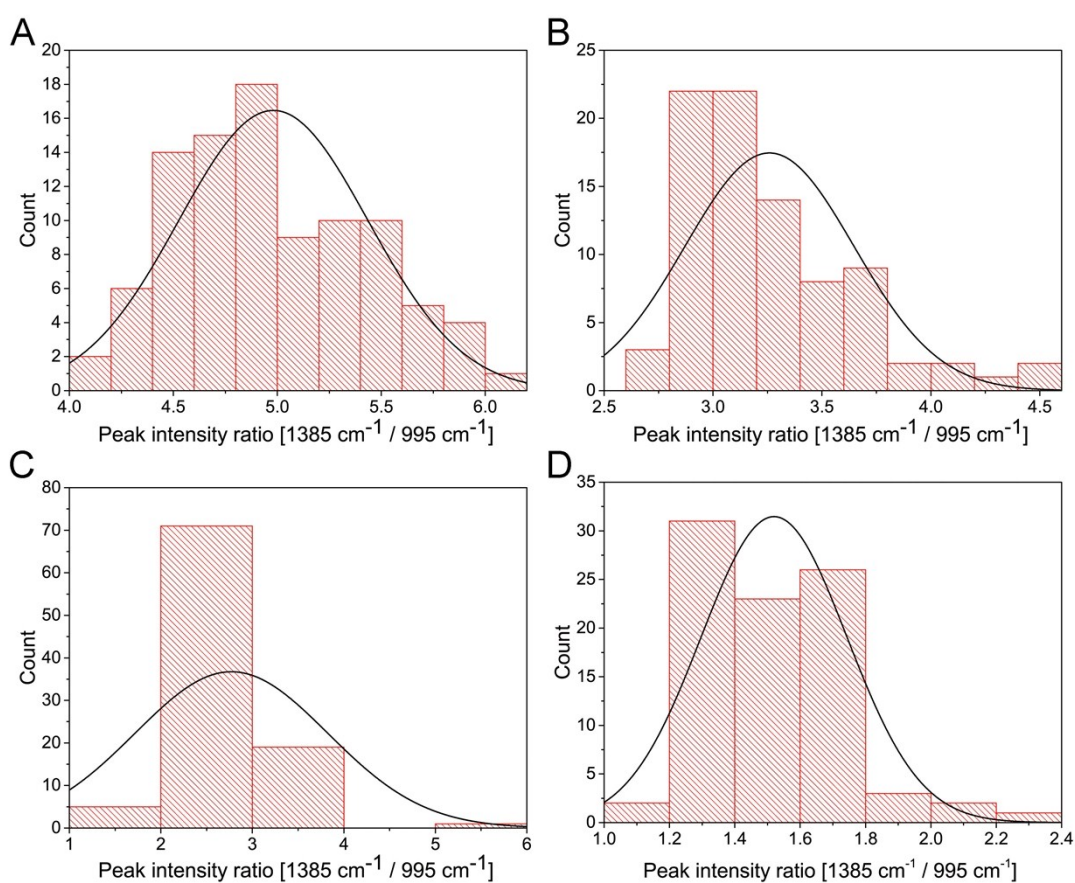


Figure S13. Peak intensity ratio between $1385\text{ cm}^{-1}/995\text{ cm}^{-1}$ distribution of the TER spectra extracted from TERS maps of monomer monolayers irradiated for different times (A. 1.5h; B.

2h; C. 5h; D. 6.5 h) The average peak intensity ratio for polymer monolayers with 1.5 h, 2h 5h and 6.5h irradiation is 4.98 with 10% variation, 3.26 with 12% variation, 2.77 with 13.5% variation and 1.52 with 13% variation, respectively.

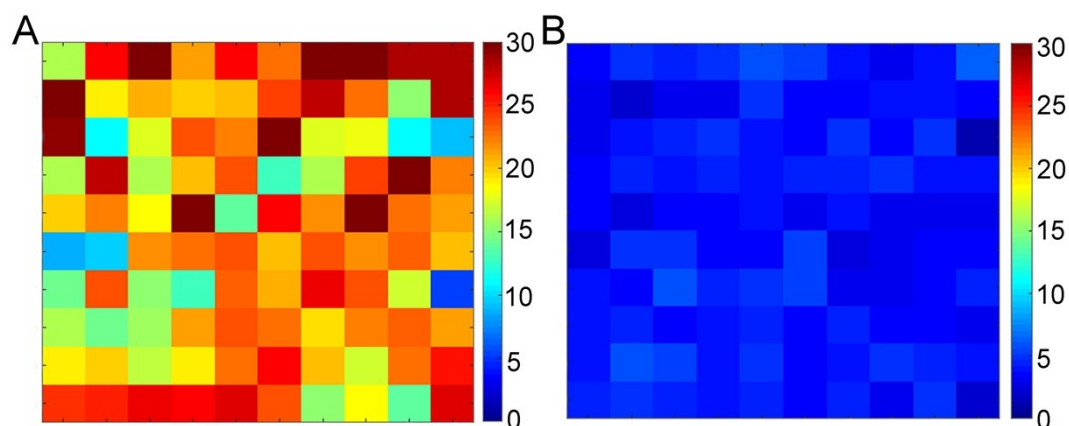


Figure S14. A. TERS peak intensity (1385 cm^{-1}) map of monomer monolayer. B. TERS peak intensity (1385 cm^{-1}) map of polymer monomer after 1.5 h UV irradiation. The size of all maps is $1 \times 1\ \mu\text{m}^2$ with a 100 nm pixel size.

Table S1. The full width at half maximum (FWHM) of the Raman peak at 1385 cm^{-1} within the TERS maps of polymer monolayers irradiated for different times.

Sample ML1	FWHM / cm^{-1}
Irradiated for 1.5 h	27.6 ± 10.6
Irradiated for 2 h	33.8 ± 16.2
Irradiated for 5 h	50.0 ± 12.4
Irradiated for 6.5 h	39.6 ± 21.0

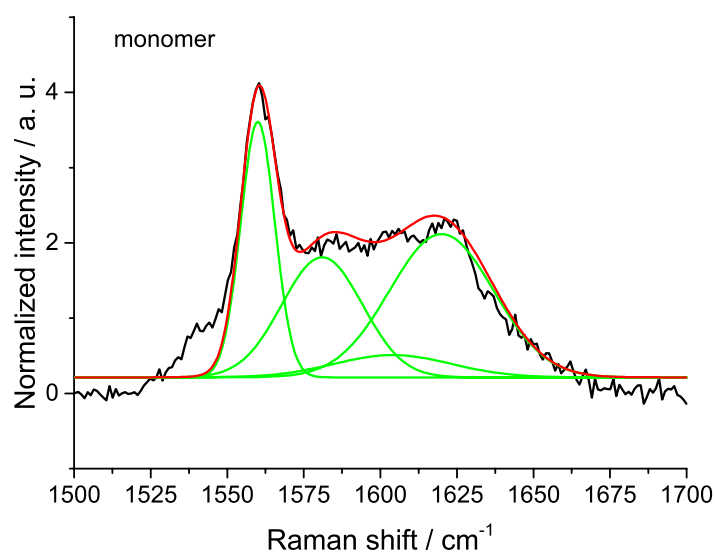


Figure S15. Gaussian fitting of the Raman peak between 1500 cm^{-1} and 1700 cm^{-1} on the average TER spectrum of monomer monolayer.

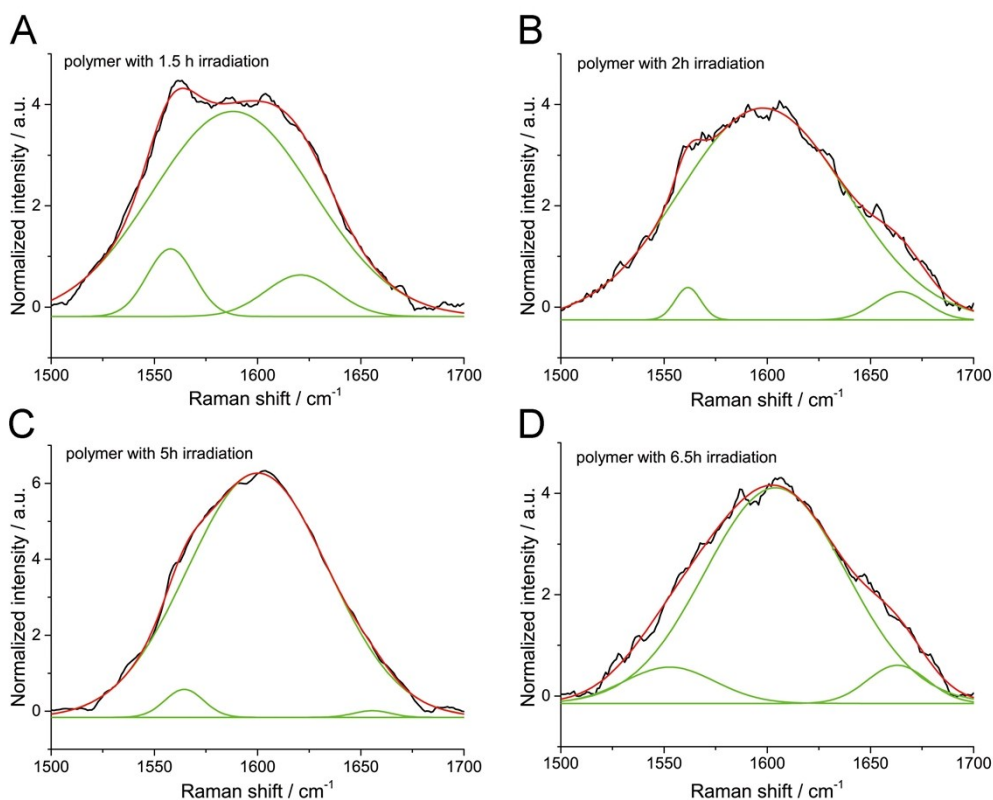


Figure S16. Gaussian fitting of the Raman peak between 1500 cm^{-1} and 1700 cm^{-1} on the average TER spectra of polymer monolayers irradiated for different times. (A. 1.5h; B. 2h; C. 5h; D. 6.5 h).

Table S2. Gaussian fitting parameters of the Raman peak between 1500 cm^{-1} and 1700 cm^{-1} on the average TER spectra of monomer monolayer and polymer monolayers irradiated for different times.

Sample ML1	Peak at 1560 cm^{-1}		Peak at 1580/1600 cm^{-1}		Peak at 1625 / 1660 cm^{-1}	
	Intensity	FWHM	Intensity	FWHM	Intensity	FWHM
Monomer	3.39	13.17	1.59	31.00	1.90	40.00
Irradiated for 1.5 h	1.33	26.88	4.05	92.06	0.82	40.15
Irradiated for 2 h	0.64	14.63	4.18	95.26	0.56	29.18
Irradiated for 5 h	0.73	22.06	6.43	80.35	0.17	21.03
Irradiated for 6.5 h	0.72	51.89	4.26	80.91	0.75	34.40

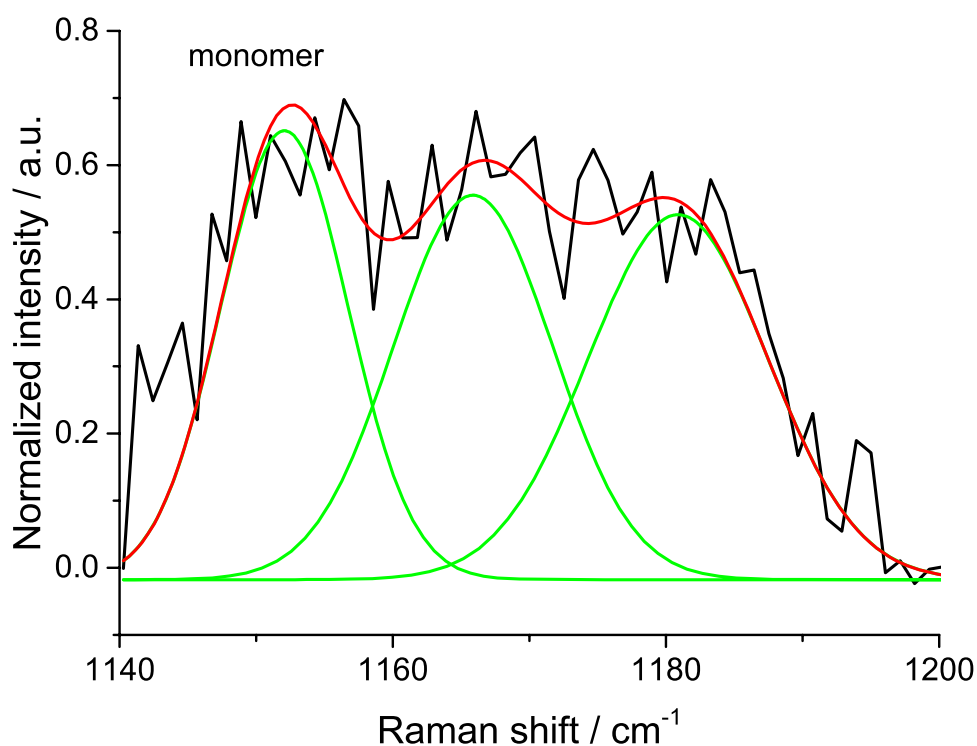


Figure S17. Gaussian fitting of the Raman peak at 1168 cm^{-1} on the average TER spectrum of monomer monolayer.

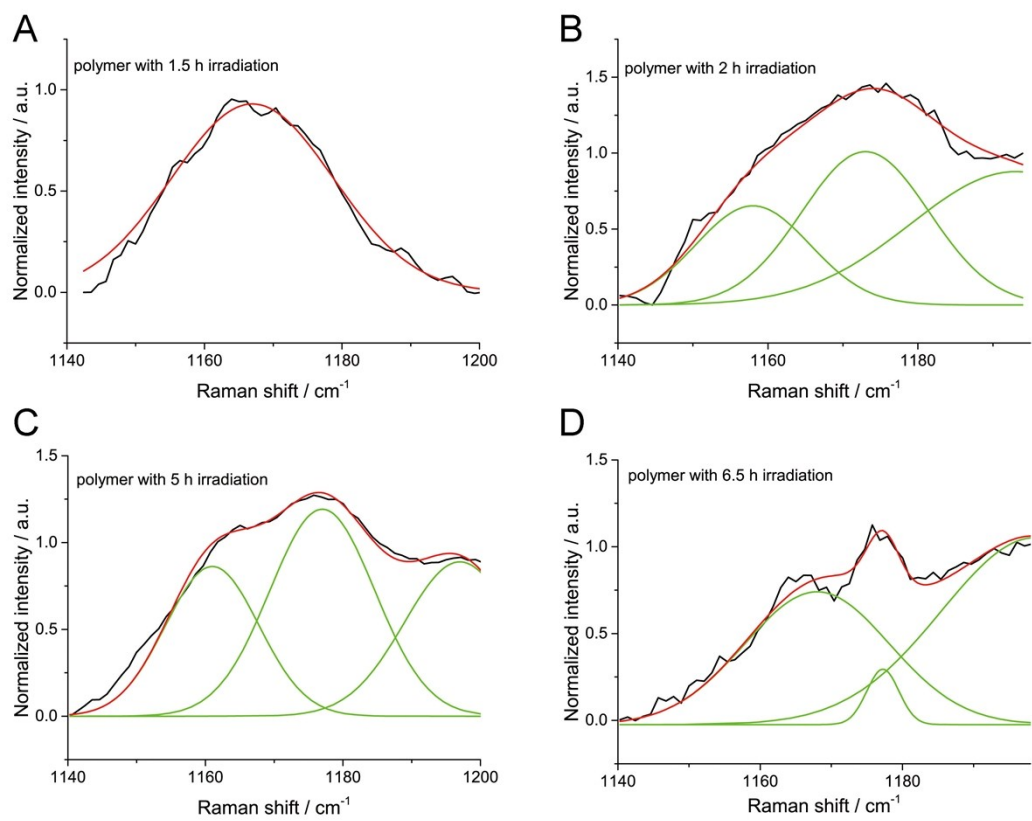


Figure S18. Gaussian fitting of the Raman peak at 1168 cm^{-1} on the average TER spectra of polymer monolayers irradiated for different times. (A. 1.5h; B. 2h; C. 5h; D. 6.5 h).

Table S3. Gaussian fitting parameters of the Raman peak at 1168 cm^{-1} in the average TER spectra of monomer monolayer and polymer monolayers irradiated for different times.

Sample ML1	Peak height	FWHM	Peak area
Not irradiated	0.57	13.7	8.3
Irradiated for 1.5 h	0.93	27.7	26.9
Irradiated for 2 h	1.01	20	30.85
Irradiated for 5 h	1.2	18	22.8
Irradiated for 6.5 h	0.74	24.0	19.5

Table S4. Gaussian fitting parameters of the Raman peak at 2215 cm^{-1} in the average TER spectra of monomer monolayer and polymer monolayers irradiated for different times.

Sample ML1	Peak height	FWHM	Peak area
Not irradiated	3.30	25.3	88.9
Irradiated for 1.5 h	5.74	33.1	202
Irradiated for 2 h	1.87	28.2	56.1
Irradiated for 5 h	1.27	32.8	44.3
Irradiated for 6.5 h	1.50	34.7	55.3

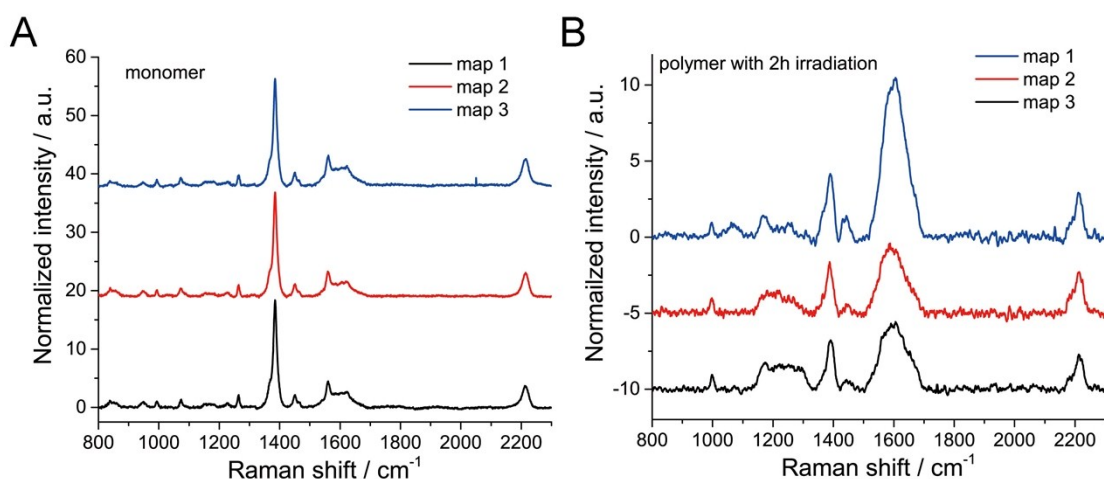


Figure S19. (A) Baseline corrected average TER spectra from three maps of a monomer monolayer at different spots. (B) Baseline corrected average TER spectra from three maps of polymer monolayers with 2h irradiation time at different spots. The size of all maps is $1 \times 1 \mu\text{m}^2$ with a 100 nm pixel size. All average TER spectra were normalized by the Raman peak of the unaffected cyclophane's central benzenes at 995 cm^{-1} .

Table S5. Peak intensity ratios between the Raman peaks at 1385 cm⁻¹ and at 995 cm⁻¹ extracted from the average TER spectra of three different TERS maps of monomer **1** monolayer (ML **1**) before and after UV irradiation for 2 h, respectively. Estimation of polymerization conversion based on them. The average TER spectra are shown in Figure S9.

Sample ML 1	Peak intensity ratio [1385 cm ⁻¹ / 995 cm ⁻¹]	Average value	Conversion [%]
Non irradiated	18.2	18.1 ± 0.115	----
	18.0		
	18.2		
Polymer irradiated for 2 h	4.13	3.58 ± 0.476	80.2 ± 2.75
	3.36		
	3.26		

Table S6. Peak intensity, area and FWHM of the Raman peaks at 1168 cm⁻¹ in the average TER spectra of three different TERS maps of monomer **1** monolayer (ML **1**) before and after UV irradiation for 2 h, respectively.

Sample ML 1	Peak intensity	Average value	Peak area	Average value	FWHM [cm ⁻¹]	Average value
Non irradiated	0.479	0.474 ± 0.050	6.16	8.10 ± 2.34	12.1	16.0 ± 3.64
	0.422		7.44		16.6	
	0.522		10.7		19.3	
Polymer irradiated for 2 h	1.20	1.07 ± 0.133	38.4	35.1 ± 3.40	30.0	30.9 ± 4.08
	0.934		35.3		35.4	
	1.08		31.6		27.4	

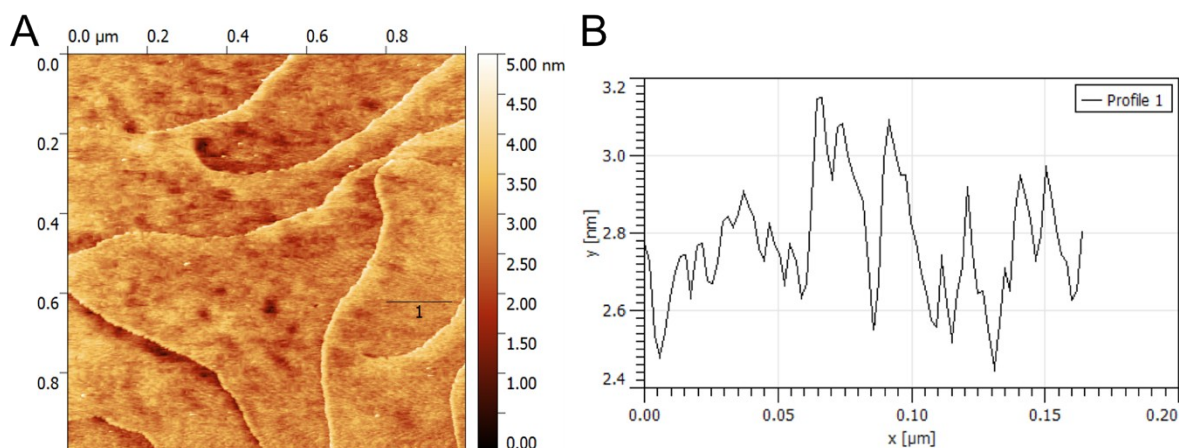


Figure S20. A. STM image of a Au (111) single crystal surface. The scan area is $1\ \mu\text{m} \times 1\ \mu\text{m}$. B. The height profile along the line indicated in the image. The tunneling conditions were 200 pA and 0.2 V. The roughness of the surface is 0.385 nm.

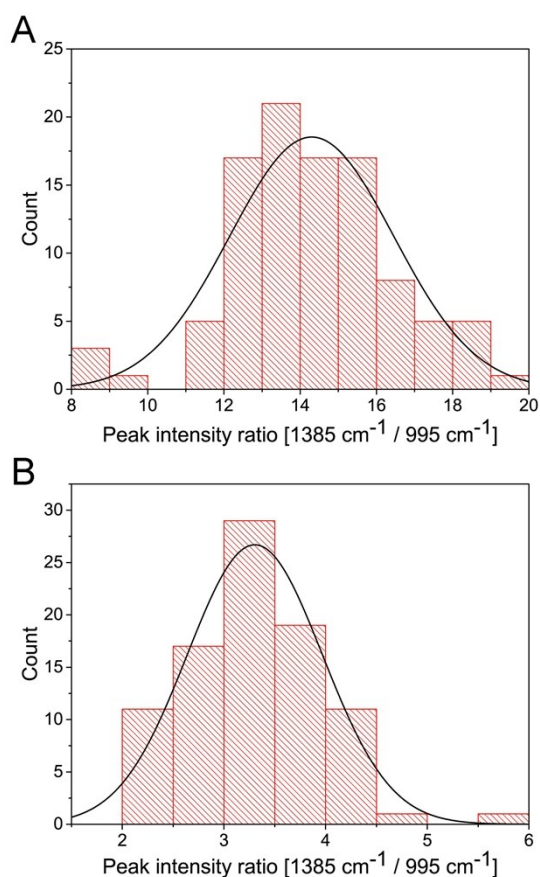


Figure S21. Peak intensity ratio between $1385\ \text{cm}^{-1}/995\ \text{cm}^{-1}$ distribution of the TERS spectra extracted from TERS maps of monomer monolayer on Au before (A) and after UV irradiation for 2.5 h (B). The average peak intensity ratio in the TERS maps of monomer before and after irradiation is 14.3 with 10 % variation and 5.37 with 12% variation, respectively.

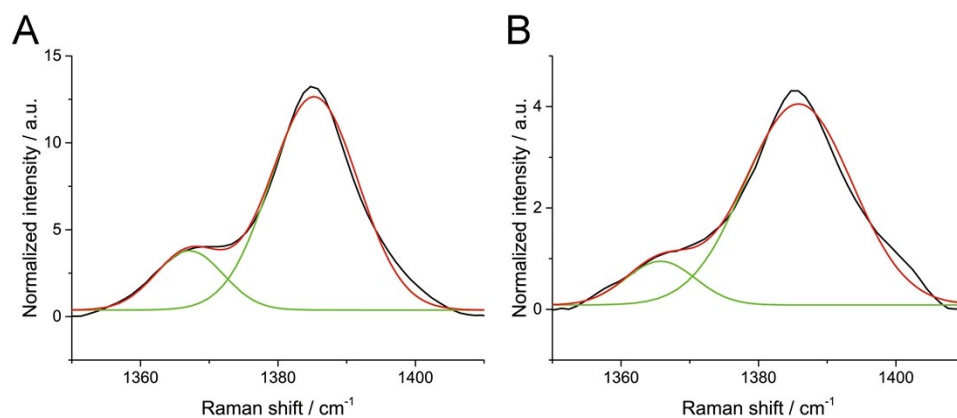


Figure S22. Gaussian fitting of the Raman shifts between 1350 cm^{-1} and 1410 cm^{-1} on the average TER spectra of monomer monolayer on Au before (A) and after (B) UV irradiation for 2.5h

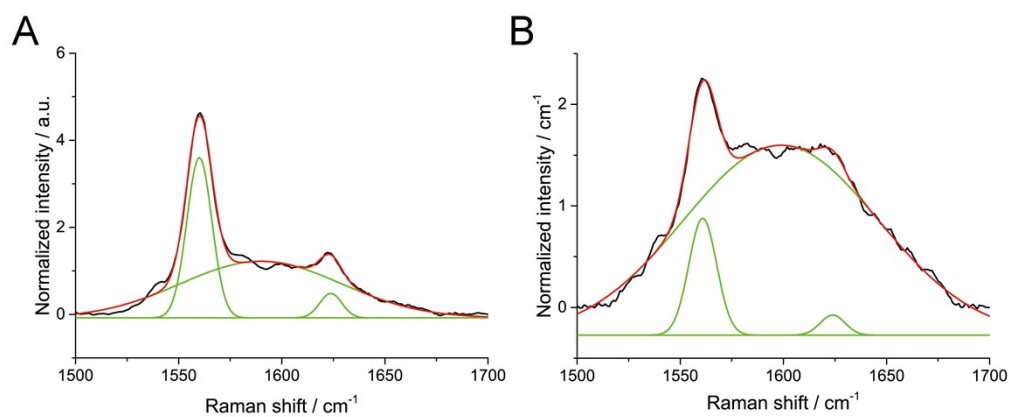


Figure S23. Gaussian fitting of the Raman peak between 1500 cm^{-1} and 1700 cm^{-1} on the average TER spectra of monomer monolayer on Au before (A) and after (B) UV irradiation for 2.5h.

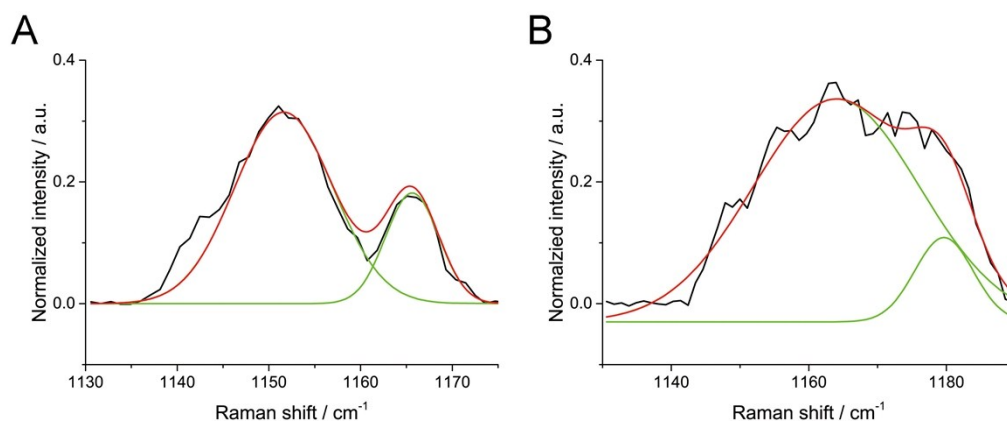


Figure S24. Gaussian fitting of the Raman peak between 1130 cm^{-1} and 1190 cm^{-1} on the average TER spectra of monomer ML on Au before (A) and after (B) irradiation for 2.5h.

Table S7. Peak intensity ratios between the anthracene peak at 1385 cm⁻¹ and ring breathing mode of the benzene ring at 995 cm⁻¹ of a monolayer of monomer **1** (ML **1**) on Au (111) before and after UV irradiation for 2.5 h.

Sample ML 1	Peak intensity ratio [1385 cm ⁻¹ / 995 cm ⁻¹]	Conversion [%]
Before irradiation	14.3 ± 1.40	
After 2.5 h irradiation	5.37 ± 0.665	62.4 ± 11.0

c. Conversion calculations

To estimate polymerization conversion, an internal standard method was taken for analysis. The intensive Raman peak at 1385 cm⁻¹ of monomer corresponds to the characteristic vibrational mode ($\nu_{(C=C)}$) of anthracene. The Raman peak at 995 cm⁻¹, which presents on both spectra of monomer and polymer, is the breathing mode of benzene ring in the middle of the monomer. This peak is basically unaffected after polymerization and was therefore selected as internal reference. Based on the intensity decrease of anthracene peak referring to the reference peak, we can estimate the polymerization degree of monomer into polymer after UV irradiation. The conversion formula is shown below:

$$\text{Conversion} = \{1 - [(I_{(1385 \text{ cm}^{-1})p} / I_{(995 \text{ cm}^{-1})p}) / (I_{(1385 \text{ cm}^{-1})m} / I_{(995 \text{ cm}^{-1})m})]\} \times 100 \% \quad (1)$$

d. Error estimation

We first subtracted the background of the spectra, smoothed them, removed the super strong peaks induced by cosmic rays, and removed those spectra whose signal-to-noise ratio is too low (< 3). Afterwards, the averaged intensity ratio $\langle N \rangle$ and the corresponding standard deviation (σ) of the Raman peaks at 1385 cm⁻¹ and at 995 cm⁻¹ in the maps were calculated and are shown in the tables. Note that, some errors caused by such data processing cannot be ignored in our calculations, which will contribute to the estimated values.

Because the intensity ratios $[I_{(1385 \text{ cm}^{-1})} / I_{(995 \text{ cm}^{-1})}]$ of monomer and polymers, R_m and R_p , are two independent variables, a formula of error propagation was applied to calculate the uncertainty of the conversion analysis mentioned above.^[6] For example, the symbols A and

B represent the results of two individual measurements, the operating result between A and B is presented as Q. The corresponding uncertainties are u_A , u_B , and u_Q .

For $Q=A\pm B$, the uncertainty of R can be expressed as follows: [6]

$$u_Q = \sqrt{(u_A)^2 + (u_B)^2} \quad (2)$$

For $Q=A\times B$ or $Q=A/B$, the uncertainty of Q can be expressed as follows: [6]

$$u_Q = Q * \sqrt{\left(\frac{u_A}{A}\right)^2 + \left(\frac{u_B}{B}\right)^2} \quad (3)$$

We used the notations of R_m and R_p to stand for the averaged peak intensity ratios of monomer and polymer, defined the true values of them using the mean values $\langle m \rangle$ and $\langle p \rangle$, and the corresponding standard deviations are σ_m and σ_p .

For the calculation of conversion,

$$C = 1 - \frac{R_p}{R_m} = \frac{R_m - R_p}{R_m} \quad (4)$$

According to the equations (2) and (3), the following equation can be obtained:

$$\begin{aligned} \frac{\sigma_C}{\langle C \rangle} &= \sqrt{\frac{\sigma_{(m-p)}^2}{(\langle m - p \rangle)^2} + \left(\frac{\sigma_m}{\langle m \rangle}\right)^2} \\ &= \sqrt{\frac{\sigma_m^2 + \sigma_p^2}{(\langle m \rangle - \langle p \rangle)^2} + \left(\frac{\sigma_m}{\langle m \rangle}\right)^2} \end{aligned} \quad (5)$$

In the end, we can get that:

$$\sigma_C = \left(\frac{\langle m \rangle - \langle p \rangle}{\langle m \rangle}\right) * \sqrt{\frac{\sigma_m^2 + \sigma_p^2}{(\langle m \rangle - \langle p \rangle)^2} + \left(\frac{\sigma_m}{\langle m \rangle}\right)^2} \quad (6)$$

We take the calculation of the conversion on a Au surface as an example. The standard deviation of the conversion can be calculated as follows:

$$\sigma_C = \left(\frac{14.3 - 5.37}{14.3}\right) * \sqrt{\frac{1.40^2 + 0.665^2}{(14.3 - 5.37)^2} + \left(\frac{1.40}{14.3}\right)^2} = 0.11 = 11 \%$$

5. References

- [1] M. Servalli, K. Celebi, P. Payamyar, L. Zheng, M. Polozij, B. Lowe, A. Kuc, T. Schwarz, K. Thorwarth, A. Borgschulte, T. Heine, R. Zenobi, A. D. Schlüter. *ACS Nano* **2018**, *12*, 11294-11306.
- [2] L. T. Banner, A. Richter, E. Pinkhassik, *Surf. Interface Anal.* **2009**, *41*, 49-55.
- [3] S. Feng, P. N. Sen, *Phys. Rev. Lett.* **1984**, *52*, 216-219.
- [4] J. Stadler, T. Schmid, R. Zenobi, *Nano Lett.* **2010**, *10*, 4514-4520.
- [5] L. Opilik, Ü. Dogan, J. Szczerbiński, R. Zenobi, *Applied Physics Letters* **2015**, *107*, 091109.
- [6] <http://www.sciencemathmastery.com/propagation-of-error-with-single-and-multiple-independent-variables/>